lutions in the concentration range 15–30 mM gave μ_{eff} of 2.7–2.9 μ_B at 298 K. Similar experiments in $(CD_3)_2SO$ yielded μ_{eff} values in the range 2.5–3.0 μ_B. These values are low for tetrahedral Ni(II) compounds. The low magnetic moment in solution of bis(iminobis(phosphine sulfido))nickel(II) (**3**) has been attributed to tetrahedral ($S = 1$) $\rightleftarrows$ planar ($S = 0$) equilibrium.[23] The temperature dependence of the solution magnetic susceptibility of the iminobis(phosphine sulfido) complex **3** indicated the diamagnetic planar species to be the favored one at lower temperatures. Since at a particular temperature, μ_{eff} values for the arenethiolates are found to be lower in more dilute (1–3 mM) solutions, it appears that the equilibrium is shifted toward the planar side even with dilution. Another possibility is polymerization into diamagnetic planar species like $[Ni_n(SAr)_{2(n+1)}]^{2-}$,[3b] following dissociation of coordinated thiolates from the paramagnetic distorted tetrahedral $[Ni(SAr)_4]^{2-}$. This possibility might also explain the appearance of weak thiolate peaks at −7 to −8 ppm in the NMR spectra of these complexes. However, addition of excess $(Et_4N)(SAr)$ to solutons of $[Ni(SAr)_4]^{2-}$ brought about hardly any change in the paramagnetically shifted resonance positions of the thiolate hydrogens reported in Table IV. This observation rules out the possibility of any equilibrium between diamagnetic multinuclear planar species and paramagnetic distorted-tetrahedral $[Ni(SAr)_4]^{2-}$ in solution. The reason(s) for lowering of μ_{eff} with dilution thus remains unclear.

The absorption spectra of 15–30 mM solutions of the complexes in acetonitrile exhibit a broad band with λ_{max} at 1800–1820 nm, a weak ($\epsilon \sim 20$ cm^{-1} M^{-1}) feature around 1280 nm and a strong absorption ($\epsilon = 650$–800 cm^{-1} M^{-1}) in the 660–680-nm region. These d–d bands are followed by intense charge-transfer bands in the 300–500-nm range. The intensity of the ~670-nm band is enhanced by overlap with high-energy charge-transfer absorption. Contrary to a previous report,[2a] extinction coefficients of the ~1800-nm band were found to be 70–120 cm^{-1} M^{-1} for fresh solutions of $[Ni(SAr)_4]^{2-}$ with no externally added thiolate. The ~1800-nm band has been assigned to $^3T_1 \rightarrow {}^3A_2$ ligand field transition of tetrahedral Ni(II).[2a,23] Thus the predominant Ni(II) species in the concentration range of NMR and magnetic susceptibility measurements is tetrahedral. The extinction coefficients of the d–d bands were found to decrease with time and on dilution. No attempt was made either to completely assign the electronic spectrum or to follow up the changes in extinction coefficients on dilution.

Summary

The following are the principal results and conclusions of this investigation.

(i) A high-yield straightforward synthetic route to tetraalkyl- and tetraarylammonium tetrakis(arenethiolato)nickelate(II) has been discovered.

(ii) The structure of $[Ni(S\text{-}p\text{-}C_6H_4Cl)_4]^{2-}$ has been determined. This structure along with the other reported briefly in a previous account demonstrates that, in $[Ni(SAr)_4]^{2-}$, the four arenethiolate ligands are arranged in a distorted tetrahedral manner. Two S–Ni–S angles are ~90° while the other four are close to 120°. Three of the four phenyl rings are coplanar with the corresponding Ni–S bonds.

(iii) On steric grounds, idealized square-planar or tetrahedral geometry for $[Ni(SAr)_4]^{2-}$ is not compatible with the tendency of the Ni–S vectors to be coplanar with the bonded phenyl rings. The observed distortion occurs to reduce steric interactions while maintaining coplanarity of Ni–S vectors and the phenyl rings. The previous suggestion of crystal packing force as the origin of such distortion seems to be highly unlikely.

(iv) The NMR spectra of several nickel arenethiolate complexes have been measured and assigned. The utility of ^1H NMR in probing paramagnetic thiolate-ligated Ni(II) sites in biological systems is apparent in the well-resolved, relatively narrow resonances exhibited by the complexes studied.

Acknowledgment. This research was supported by a Faculty Research Committee Grant at the University of California, Santa Cruz. We thank S. Swedberg for help in the initial synthetic attempts and Dr. F. Hollander for experimental assistance in crystal structure determination.

Registry No. **1**, 103003-19-6; $(Et_4N)_2[Ni(SC_6H_5)_4]$, 93841-89-5; $(Ph_4P)_2[Ni(SC_6H_5)_4]$, 57927-74-9; $(Et_4N)_2[Ni(S\text{-}m\text{-}C_6H_4Cl)_4]$, 103024-60-8; $(Et_4N)_2[Ni(S\text{-}p\text{-}C_6H_4CH_3)_4]$, 103003-21-0; $(Et_4N)_2NiCl_4$, 5964-71-6.

Supplementary Material Available: Thermal parameters of cations and the anion (Table S1) and positional and thermal parameters for hydrogen atoms of $(Et_4N)_2[Ni(S\text{-}p\text{-}C_6H_4Cl)_4]$ (Table S2) (4 pages). Ordering information is given on any current masthead page.

Contribution from the Department of Applied Chemistry, Faculty of Engineering, Osaka University, Suita, Osaka 565, Japan

Assimilatory and Dissimilatory Reduction of NO_3^- and NO_2^- with an $(n\text{-}Bu_4N)_3[Mo_2Fe_6S_8(SPh)_9]$ Modified Glassy-Carbon Electrode in Water

Susumu Kuwabata, Satoshi Uezumi, Koji Tanaka, and Toshio Tanaka*

Received January 2, 1986

The catalytic reduction of NO_3^- to NH_3 with an $(n\text{-}Bu_4N)_3[Mo_2Fe_6S_8(SPh)_9]$ modified glassy-carbon ([Mo-Fe]/GC) electrode has been accomplished for the first time by the controlled-potential electrolysis at −1.25 V vs. SCE in water. The current efficiency for the formation of NH_3 is 80.3% at pH 10. Not only NO_2^- but also NH_2OH were detected as reaction intermediates, and both of them are reduced to NH_3 quite easily under the same conditions. On the other hand, the reduction of NO_2^- with the same electrode at −1.10 V vs. SCE results in the evolution of N_2O without producing NH_3. Thus, the assimilatory reductions of NO_3^- and NO_2^- giving NH_3 take place when both substrates are reduced with the [Mo-Fe]/GC electrode at −1.25 V vs. SCE, whereas the dissimilatory reduction of NO_2^- affording N_2O selectively occurs in the electrochemical reduction of NO_2^- conducted at −1.10 V vs. SCE.

Introduction

The amounts of N_2, NH_3, NO_2^-, and NO_3^- in the natural world have been regulated by the nitrogen cycle (Scheme I).[1,2] Among those inorganic nitrogen molecules, only ammonia can be converted into organic nitrogen molecules in the metabolisms. Most of the higher plants and microorganisms that are not provided with the ability of N_2 fixation, therefore, reduce NO_3^- and NO_2^- to produce NH_3 (assimilatory reductions).[3] On the other hand, various denitrification bacteria reduce NO_3^- and NO_2^- to N_2O, which is further reduced to N_2 (dissimilatory reductions).[3-7] The latter

(1) Hughes, M. N. *The Inorganic Chemistry of Biological Processes*; Wiley: New York, 1981.
(2) Doelle, H. W. *Bacterial Metabolism*; Academic: New York, 1969.
(3) Payne, W. J. *Bacteriol. Rev.* **1973**, *409*, 1973 and references therein.

0020-1669/86/1325-3018$01.50/0

Scheme I

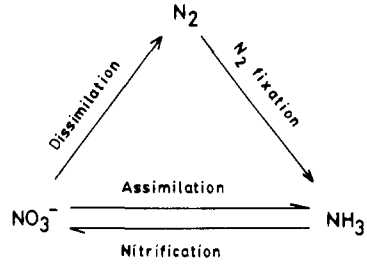

species are particularly of interest in biological removal of NO_3^- and NO_2^- from the water of rivers and lakes.

Molybdenum is considered as an active site in nitrate reductases which reduce NO_3^- to NO_2^-,[8-12] and the latter is further reduced to NH_3 and N_2 by assimilatory and dissimilatory nitrite reductases, respectively. Previous model studies on nitrate reductases have shown that the reduction of NO_3^- with molybdenum complexes affords a variety of products such as NO_2, NO_2^-, NO, N_2O, NH_3OH^+, and NH_4^+, depending on the reaction conditions.[13-21] It has recently been shown that NO_2^- is reduced catalytically to NH_3 and N_2O by iron(II) porphyrin[22] and $MoO_2(S_2CNEt_2)_2$,[23] respectively. With respect to the reduction of NO_3^-, a cathodic current of a Pt electrode has been confirmed to increase with an increase in the concentration of NO_3^- in water, but the product of the reduction has not been identified.[24] Recently, we have briefly reported the catalytic multielectron reduction of NO_3^- (eq 1) by the use of an $(n\text{-}Bu_4N)_3[Mo_2Fe_6S_8(SPh)_9]$ modified

$$NO_3^- + 9H^+ + 8e^- \rightarrow NH_3 + 3H_2O \qquad (1)$$

glassy-carbon ([Mo-Fe]/GC) electrode.[25] This paper reports the catalytic reductions of NO_3^- to NH_3 and NO_2^- to N_2O by a [Mo-Fe]/GC electrode in water.

Experimental Section

Materials. Commercially available guaranteed reagent grades of $NaNO_3$, $NaNO_2$, H_3PO_4, NaOH, and NH_2OH were used without further purification. $(n\text{-}Bu_4N)_3[Mo_2Fe_6S_8(SPh)_9]$, ($(n\text{-}Bu_4N)_3$[Mo-Fe]),[26,27]

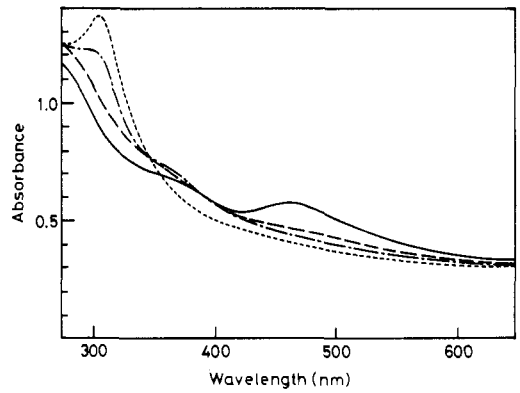

Figure 1. Electronic absorption spectra of $(n\text{-}Bu_4N)_3$[Mo-Fe] (2.0×10^{-4} mol dm^{-3}) (—) and the reduced species $[Mo\text{-}Fe]^{4-}$ produced at −1.10 V vs. SCE in the absence of either NO_3^- or NO_2^- (– – –), in the presence of $(Et_4N)NO_3$ (2.0×10^{-3} mol dm^{-3}) (–·–), and in the presence of $(n\text{-}Bu_4N)NO_2$ (2.0×10^{-3} mol dm^{-3}) (– ·· –), in DMF.

$(n\text{-}Bu_4N)NO_2$,[21] and $(Et_4N)NO_3$[16] were prepared according to the literature. Solvents used for electrochemical measurements were purified by distillation over appropriate desiccants, DMF from CaH_2 under reduced pressure and CH_3CN from P_2O_5, and stored under an N_2 atmosphere. Immediately before use they were bubbled with He for at least 1 h to remove dinitrogen dissolved in the solvents.

Preparation of an $(n\text{-}Bu_4N)_3$[Mo-Fe] Modified Glassy-Carbon ([Mo-Fe]/GC) Electrode. Glassy-carbon plates with areas of 1.0 and 3.0 cm^2 (Tokai Carbon Co. Ltd., SC-2) were polished well with Al_2O_3 (0.3 μm) and washed with distilled water several times. Copper-wire electrical leads were attached with silver epoxy to the back of the polished glassy-carbon plate, and then the back and round rims of the glassy-carbon plates were coated with epoxy resin. A given amount of an acetonitrile solution of $(n\text{-}Bu_4N)_3$[Mo-Fe] (1.0×10^{-3} mol dm^{-3}) was dropped on a polished surface of the glassy-carbon plates by a syringe technique and dried for ca. 30 min under a dry N_2 stream. The [Mo-Fe]/GC electrodes with surface areas of 1.0 and 3.0 cm^2 thus prepared were used for electrochemical measurements and the reduction of NO_2^- or NO_3^-, respectively.

A rotating ring-disk electrode (RRDE) with an $(n\text{-}Bu_4N)_3$[Mo-Fe] modified disk moiety was used in order to detect intermediates in the reduction of NO_2^-. A glassy-carbon pipe (7-mm outside diameter, 5-mm inside diameter, and 8-mm length; Tokai Carbon Co. Ltd., P-5-100) was attached with epoxy resin around a glassy-carbon-disk electrode (3-mm diameter) mounted in a glass tube (5-mm diameter; Yanagimoto MGF Co. Ltd., GC-P2). A copper-wire electrical lead was attached to the inside of the glassy-carbon ring with silver epoxy and epoxy resin. Then, the outside of the ring electrode was mounted in a glass tube (7-mm diameter) with epoxy resin. The disk electrode was modified with $(n\text{-}Bu_4N)_3$[Mo-Fe] by the same way as described above. The RRDE was used at 1000 rpm by a rotating electrode head (Yanagimoto MGF Co. Ltd., P-10-RE).

Physical Measurements. Electronic absorption spectra were measured with a Union SM-401 spectrophotometer. Spectroelectrochemical experiments were carried out by the use of an optically transparent thin-layer electrode (OTTLE)[28] consisting of a Pt-gauze electrode in a 0.5 mm width quartz cuvette, a Pt-wire auxiliary electrode, and a saturated calomel electrode (SCE) as a reference. All the electrochemical measurements of [Mo-Fe]/GC were conducted in water containing an H_3PO_4–NaOH buffer (0.2 mol dm^{-3}) placed in a Pyrex cell equipped with a Pt auxiliary electrode, an SCE, and a nozzle for bubbling N_2 or He. Cyclic voltammograms and RRDE curves were obtained by the use of a Hokuto Denko HB-401 potentiostat, a Hokuto Denko HB-107A function generator, and a Yokogawa Electric, Inc., 3077 X-Y recorder.

Reduction of NO_3^-, NO_2^-, and NH_2OH. The reductions of NO_3^-, NO_2^-, and NH_2OH with the [Mo-Fe]/GC electrode in water were carried out under controlled-potential electrolysis conditions with an electrolysis cell consisting of three components as described in a previous paper.[29] A cation membrane (Nafion film) was used as a separator between the [Mo-Fe]/GC working electrode and the Pt-plate counter electrode compartments. After He was passed through the electrolysis cell for at least 1 h to remove air, an aqueous solution containing $NaNO_3$,

(4) Payne, W. J.; Grant, M. A. *Basic Life Sci.* **1981**, *17*, 411.
(5) Payne, W. J. *Denitrification*; Wiley: New York, 1981.
(6) Krowles, R. *Microbiol. Rev.* **1982**, *46*, 43.
(7) Iwasaki, H.; Shidara, S.; Suzuki, H.; Mori, T. *J. Biochem. (Tokyo)* **1963**, *53*, 299.
(8) Spence, J. T. *Arch. Biochem. Biophys.* **1970**, *137*, 287.
(9) Nicholas, D. J. D.; Stevens, H. M. *Nature (London)* **1955**, *176*, 1066.
(10) Bray, R. C.; Swann, J. C. *Struct. Bonding (Berlin)* **1972**, *11*, 107.
(11) Forget, P.; Dervartanian, D. V. *Biochim. Biophys. Acta* **1972**, *256*, 600.
(12) Dervartanian, D. V.; Forget, P. *Biochim. Biophys. Acta* **1975**, *379*, 74.
(13) Haight, G. P.; Mohilner, P.; Katz, A. *Acta Chem. Scand.* **1962**, *16*, 221.
(14) Haight, G. P.; Alfred, K. *Acta Chem. Scand.* **1962**, *16*, 659.
(15) Taylor, R. D.; Spence, J. T. *Inorg. Chem.* **1975**, *14*, 2815.
(16) Garner, C. D.; Hyde, M. R.; Mabbs, F. E.; Routledge, V. I. *J. Chem. Soc., Dalton Trans.* **1975**, 1180.
(17) Garner, C. D.; Hyde, M. R.; Mabbs, F. E. *Inorg. Chem.* **1976**, *15*, 2327.
(18) Garner, C. D.; Hyde, M. R.; Mabbs, F. E. *Inorg. Chem.* **1977**, *16*, 2122.
(19) Taylor, R. D.; Todd, R. G.; Chasteen, N. D.; Spence, F. T. *Inorg. Chem.* **1979**, *18*, 44.
(20) Topich, J. *Inorg. Chim. Acta* **1980**, *46*, L97.
(21) Hyde, M. R.; Garner, C. D. *J. Chem. Soc., Dalton Trans.* **1975**, 1186.
(22) Barley, M. H.; Takeuchi, K.; Murphy, W. R., Jr.; Meyer, T. J. *J. Chem. Soc., Chem. Commun.* **1985**, 507.
(23) Tanaka, K.; Honjo, M.; Tanka, T. *Inorg. Chem.* **1985**, *24*, 2662.
(24) Horaryi, G.; Rizmayer, E. M. *J. Electroanal. Chem. Interfacial Electrochem.* **1985**, *188*, 265.
(25) Kuwabata, S.; Uezumi, S.; Tanaka, K.; Tanaka, T. *J. Chem. Soc., Chem. Commun.* **1986**, 135.
(26) Christou, G.; Garner, C. D. *J. Chem. Soc., Dalton Trans.* **1980**, 2354.
(27) Christou, G.; Garner, C. D.; Miller, R. M. *J. Chem. Soc., Dalton Trans.* **1980**, 2363.
(28) Lexa, D.; Savene, J. M.; Zickler, J. *J. Am. Chem. Soc.* **1977**, *99*, 786.
(29) Tanaka, K.; Honjo, M.; Tanaka, T. *J. Inorg. Biochem.* **1984**, *22*, 1873.

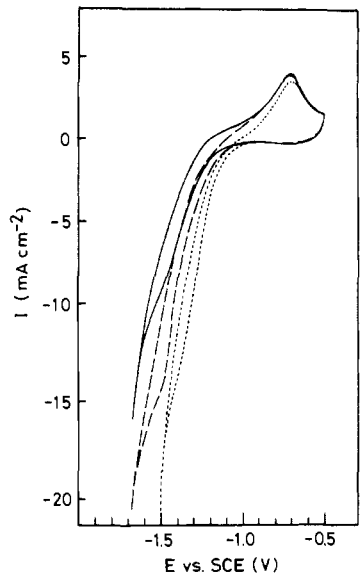

Figure 2. Cyclic voltammograms of $[Mo\text{-}Fe]^{3-}$ modified on a glassy-carbon electrode in the absence of either NO_3^- or NO_2^- (—), in the presence of $NaNO_3$ (5.0×10^{-2} mol dm^{-3}) (– – –), and in the presence of $NaNO_2$ (5.0×10^{-2} mol dm^{-3}) (- - -), in aqueous H_3PO_4–NaOH buffer solutions at pH 10 (dE/dt = 100 mV s^{-1}).

$NaNO_2$, or NH_2OH and an H_3PO_4–NaOH buffer was introduced into each electrode compartment by syringe techniques. Then, the electrolysis cell was placed in a thermostat at 30 ± 0.1 °C and the reduction of substrates was started by applying a fixed potential to the [Mo-Fe]/GC electrode with a potentiostat. The charge consumed in the reduction was measured with a Hokuto Denko HF-201 coulometer. Analyses of H_2 and N_2O evolved in the reduction were conducted on a Shimadzu GC-3BT gas chromatograph with a 2.0-m column filled with 13X molecular sieves and a Shimadzu GC-7A gas chromatograph with Porapak Q, respectively. Ammonia and NO_2^- produced in solution were determined by a Shimadzu GC-6A gas chromatograph with Chromosorb 103 and by colorimetric titration,[30] respectively.

Results and Discussion

Interaction of $[Mo\text{-}Fe]^{3-}$ with NO_3^- and NO_2^-. The electronic absorption spectrum of $(n\text{-}Bu_4N)_3[Mo\text{-}Fe]$ in DMF shows two absorption bands at 360 and 460 nm as shown by a solid line in Figure 1. The spectrum does not change at all upon the addition of $(Et_4N)NO_3$ or $(n\text{-}Bu_4N)NO_2$ to the DMF solution, whereas the controlled-potential electrolysis of the solution at −1.10 V vs. SCE in the presence of either the NO_3^- or the NO_2^- salt results in the appearance of a new band at 306 nm, accompanied by disappearance of the 460-nm band (dotted-broken and dashed lines for NO_3^- and NO_2^-, respectively, in Figure 1), which is markedly different from the spectrum of $[Mo\text{-}Fe]^{4-}$ (broken line in Figure 1) prepared under controlled-potential electrolysis at −1.10 V vs. SCE in the absence of such a substrate. The 306-nm band is assigned to the PhS^- anion, which is liberated from the cluster, since the band position and the feature coincide with those of the spectrum of PhS^- prepared by the electrochemical reduction of PhSH at −1.50 V vs. SCE in DMF.[31] It is well-known that terminal thiolate ligands of double-cubane molybdenum–iron–sulfur clusters are labile to undergo substitution reactions, whereas bridging ligands are inert to such reactions.[32] These results strongly suggest that the reduced species of the cluster undergoes substitution reactions by NO_3^- and NO_2^- at the terminal phenylthiolate ligand. The rise of the absorbance at 306 nm in the presence of NO_3^- continued over a period of 1 h, while in the presence of NO_2^- it was completed in 15 min. In addition, the final absorptivity of the 306-nm band in the presence of NO_3^- is about half of that in the presence of NO_2^-. Thus, the interaction of NO_2^- with the reduced form of the cluster is fairly stronger than that of NO_3^-. It should, however, be noted that such adduct formations take place only with the reduced form of the cluster, since the reoxidation of the cluster at −0.6 V vs. SCE resulted in regeneration of the spectrum of $[Mo\text{-}Fe]^{3-}$ in 30 min even in the presence of NO_3^- or NO_2^-.

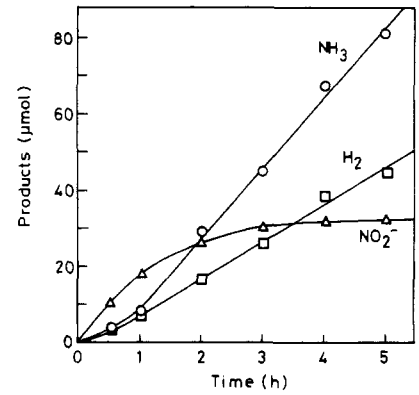

Figure 3. Reduction of NO_3^- (5.0×10^{-2} mol dm^{-3}) catalyzed by a $(n\text{-}Bu_4N)_3[Mo\text{-}Fe]$ (1.0×10^{-7} mol) modified glassy-carbon electrode (3 cm^2) under electrolysis conditions at −1.25 V vs. SCE in an aqueous H_3PO_4–NaOH buffer (0.2 mol dm^{-3}) solution (pH 10).

Cyclic Voltammograms of $[Mo\text{-}Fe]^{3-}$ Modified on a Glassy-Carbon Electrode in the Presence of NO_3^- or NO_2^- in Water. The cyclic voltammogram (CV) of the [Mo-Fe]/GC electrode in water at pH 10 (a solid line in Figure 2) shows a cathodic wave due not only to the reduction of $[Mo\text{-}Fe]^{3-}$ modified on a glassy-carbon electrode but also to the evolution of H_2 catalyzed by the reduced species of the cluster[33] at potentials more negative than −1.1 V vs. SCE, and an anodic wave around −0.7 V vs. SCE in the reverse scan. The coulomb consumed in the anodic wave was 2e/mol of $[Mo\text{-}Fe]^{3-}$ modified on a glassy-carbon electrode suggesting that $[Mo\text{-}Fe]^3$ undergoes two-electron reduction at potentials more negative than −1.10 V vs. SCE. In addition, the cyclic voltammogram was essentially unchanged even with multiscanning for 2 h. On the other hand, the cyclic voltammograms of $[Mo\text{-}Fe]^{3-}$ modified on glassy carbon in water (pH 10) in the presence of 5.0×10^{-2} mol dm^{-3} of $NaNO_3$ (a broken line in Figure 2) and $NaNO_2$ (a dotted line in Figure 2) demonstrate a remarkable increase of the cathodic current compared with that in the absence of either substrate; the current densities at −1.25 V vs. SCE in the presence of NO_3^- and NO_2^- are 2 and 5 times larger than that in the absence of them, respectively, suggesting that both substrates are reduced with the [Mo-Fe]/GC electrode and NO_2^- undergoes the reduction more easily than NO_3^-.[34] This is consistent with the assumption that the reduced species of $[Mo\text{-}Fe]^{3-}$ can interact with NO_2^- more strongly than with NO_3^- as described above.

Reduction of NO_3^- with the [Mo-Fe]/GC Electrode. It has been reported that $[Mo\text{-}Fe]^{5-}$ reacts with PhSH to evolve H_2 in DMF. In accordance with this, the controlled-potential electrolysis of $(n\text{-}Bu_4N)_3[Mo\text{-}Fe]$ (27.0 μmol) at −1.25 V vs. SCE with a glassy-carbon electrode in DMF (27 cm^3) containing PhSH (1.35 mmol) and $n\text{-}Bu_4NClO_4$ (2.70 mmol) catalytically produced H_2 with a current efficiency of almost 100%, and the amount of H_2 evolved was 98.3 μmol in 6 h. The rate of the H_2 evolution was not changed at all even when the electrolysis was conducted in the presence of $NaNO_3$ (1.35 mmol) under the same conditions, and no reduction products of NO_3^- were formed in the electrolysis in 6 h. As mentioned above, the molybdenum–iron cluster forms an adduct with NO_3^- with liberation of a terminal PhS^- ligand. The presence of a large excess of PhSH as a proton source may, therefore, prevent the formation of the NO_3^- cluster adduct, suggesting that PhSH is not adequate for the proton source in the reduction of NO_3^-.

(30) Shinn, M. B. *Ind. Eng. Chem., Anal. Ed.* **1941**, *13*, 33.
(31) Bradbury, J. R.; Hanson, G. R.; Boyd, I. W.; Gheller, S. F.; Wedd, A. G.; Murry, K. S.; Bond, A. M. *Chem. Uses Molybdenum* **1979**, *3*, 300.
(32) Palermo, R. E.; Power, P. P.; Holm, R. H. *Inorg. Chem.* **1982**, *21*, 173.
(33) No H_2 evolution occurs on the glassy-carbon electrode at potentials more positive than −1.7 V vs. SCE at pH 10.0.
(34) A glassy-carbon electrode polished with alumina reduces neither NO_3^- nor NO_2^- at potentials more positive than −1.80 V vs. SCE in water at pH 10.0.

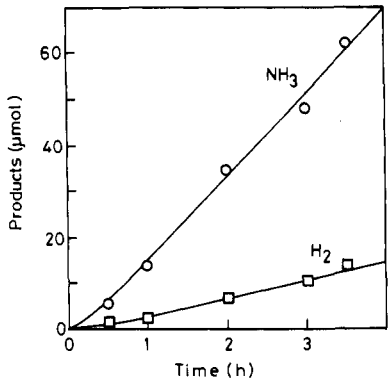

Figure 4. Reduction of NO_2^- (5.0×10^{-3} mol dm^{-3}) catalyzed by a $(n\text{-}Bu_4N)_3$[Mo-Fe] (1.0×10^{-7} mol) modified glassy-carbon electrode (3 cm^2) under electrolysis conditions at −1.25 V vs. SCE in an aqueous $NaOH-H_3PO_4$ buffer (0.2 mol dm^{-3}) solution (pH 10).

We have recently demonstrated that the [Mo-Fe]/GC electrode is activated by a dissociation of PhS^- from the cluster toward the reduction of alkyl azides.[35] In fact, the reduction of NO_3^- with the [Mo-Fe]/GC electrode in water at pH 10 catalytically produces NO_2^-, NH_3, and H_2 under controlled-potential electrolysis at −1.25 V vs. SCE, as shown in Figure 3, which indicates that the amount of NO_2^- formed increases with time in the initial 3 h but thereafter remains almost constant. On the other hand, NH_3 linearly increases in the amount with time after the lapse of about 1 h. The saturation of the formation of NO_2^- and the presence of an induction period for the formation of NH_3 manifest that at first NO_3^- is reduced to NO_2^- with two electrons, followed by a six-electron reduction affording NH_3 (eq 2). The current

$$NO_3^- \xrightarrow[2H^+ \quad H_2O]{2e^-} NO_2^- \xrightarrow[7H^+ \quad 2H_2O]{6e^-} NH_3 \qquad (2)$$

efficiencies for the formation of NO_2^-, NH_3, and H_2 were 7.7, 80.3, and 11.3%, respectively, in 5 h, suggesting that only the reductions of NO_3^- and protons take place under the present conditions. Thus, the molybdenum–iron–sulfur cluster modified on a glassy-carbon electrode efficiently reduces NO_3^- in water. This was confirmed also in the following experiment. After the reduction of NO_3^- with the [Mo-Fe]/GC electrode[36] at −1.25 V vs. SCE in water at pH 10.0 in 4 h, PhSH (30 μmol) was added to the aqueous phase. The potential of the [Mo-Fe]/GC electrode was shifted to −0.50 V vs. SCE and maintained for 20 min in order not only to oxidize the cluster but also to force the free PhSH to coordinate to the cluster since the reduced species of the cluster forms an adduct with NO_3^- and NO_2^- with liberation of a terminal PhS^- ligand. Then, the [Mo-Fe]/GC electrode was taken out of the electrolysis cell, washed with distilled water several times, and dried under a stream of N_2. The molybdenum–iron–sulfur cluster was extracted with a DMF solution (5 cm^3) of $n\text{-}Bu_4NClO_4$ (0.1 mol dm^{-3}) from the [Mo-Fe]/GC electrode. The cyclic voltammogram of this solution was consistent not only with the peak potentials of the $[Mo\text{-}Fe]^{3-/4-}$ and the $[Mo\text{-}Fe]^{4-/5-}$ redox couples (E_{pc} = −1.06 and −1.26 V and E_{pa} = −0.99 and −1.19 V vs. SCE) but also with the peak currents of those redox couples of $(n\text{-}Bu_4N)_3$[Mo-Fe] in DMF (1.0 mmol dm^{-3}). Thus, the molybdenum–iron–sulfur cluster modified on a glassy-carbon plate does not undergo a degradation reaction during the reduction of NO_3^-.

Reduction of NO_2^- with the [Mo-Fe]/GC Electrode. In order to obtain more detailed information about the reduction of NO_3^- to NH_3, the reduction of NO_2^- with the [Mo-Fe]/GC electrode was carried out under the same electrolysis conditions as for the reduction of NO_3^-. As mentioned in the previous section, the reduction of NO_2^- with the [Mo-Fe]/GC electrode is much easier than that of NO_3^-. In fact, the multielectron reduction of NO_2^- smoothly proceeds to produce NH_3 (eq 3) together with H_2, with

$$NO_2^- + 7H^+ + 6e^- \rightarrow NH_3 + 2H_2O \qquad (3)$$

no induction period, as shown in Figure 4; even when the concentration of $NaNO_2$ in solution is one-tenth of that of NO_3^-, the formation rate of NH_3 is still faster than that in the reduction of NO_3^- (compare Figure 4 with Figure 3). Moreover, no products other than H_2 and NH_3 have been confirmed in the reduction, and the current efficiency for the formation of NH_3 was 88.9%.

An RRDE technique was applied for the detection of intermediates involved in the reduction of NO_2^- to NH_3 in water. The current (I_d)–potential (E_d) curve at the [Mo-Fe]/GC-disk electrode in the presence of NO_2^- (5.0×10^{-1} mol dm^{-3}) at pH 10 is shown in Figure 5 (curve a), which exhibits an increase of I_d at potentials more negative than −1.1 V vs. SCE owing to the reductions of NO_2^- and protons. Then, the ring electrode, being maintained at E_r = 0.5 V vs. SCE (E_r = ring-electrode potential) detects an increase of the anodic ring current, I_r, when the disk-electrode potential E_d is moved negatively (Figure 5). The anodic ring current apparently results from the oxidation of a reduction intermediate, since electrochemical oxidations of H_2, NH_3, and NO_2^- have not occurred to detectable extents on a glassy-carbon ring electrode at +0.5 V vs. SCE. Figure 6 shows the I_r–E_r curves for an aqueous H_3PO_4–NaOH buffer solution of $NaNO_2$ at E_d = −0.6 and −1.5 V vs. SCE. No electrochemical reduction of NO_2^- occurs on the [Mo-Fe]/GC-disk electrode at E_d = −0.6 V vs. SCE, as deduced from curve a in Figure 5. The increase of I_r at positive ring potential E_r more than +0.5 V vs. SCE when E_d = −0.6 V vs. SCE (a broken line in Figure 6) may be caused by the oxidation of NO_2^- to NO_3^- at the glassy-carbon-ring electrode. On the other hand, the I_r–E_r curve moves

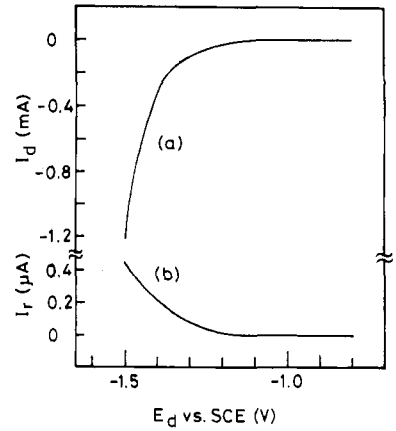

Figure 5. Current curves of the disk (a) and the ring (b) electrodes vs. potentials of the disk electrode (0.071 cm^2) modified with $(n\text{-}Bu_4N)_3$[Mo-Fe] (5.6×10^{-8} mol) in an aqueous H_3PO_4–NaOH solution (0.2 mol dm^{-3}) containing $NaNO_2$ (0.1 mol dm^{-3}). The potential of the ring electrode is +0.5 V (vs. SCE); dE/dt = 10 mV s^{-1}, and ω = 1000 rpm.

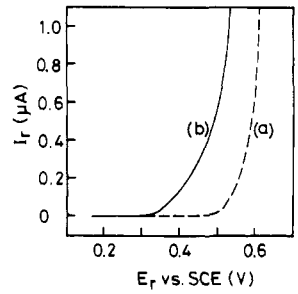

Figure 6. Current vs. potential curves for the ring electrode in an aqueous H_3PO_4–NaOH buffer solution (0.2 mol dm^{-3}) containing $NaNO_2$ (0.1 mol dm^{-3}). The potential of a disk electrode modified with $(n\text{-}Bu_4N)_3$[Mo-Fe] (5.6×10^{-8} mol) is −0.6 V (a) and −1.5 V (b) vs. SCE; dE/dt = 10 mV s^{-1}, and ω = 1000 rpm.

(35) Kuwabata, S.; Tanaka, K.; Tanaka, T. *Inorg. Chem.* **1986**, *25*, 1691.
(36) In order to obtain a reliable cyclic voltammogram of the molybdenum–iron–sulfur cluster extracted from the [Mo-Fe]/GC electrode, 5×10^{-6} mol of $(n\text{-}Bu_4N)_3$[Mo-Fe] was modified on the glassy-carbon plate (3.0 cm^2) in this experiment.

Table I. Reductions of $NaNO_3$, $NaNO_2$, and NH_2OH Catalyzed by $(n\text{-}Bu_4N)_3[Mo\text{-}Fe]^a$ Modified on a Glassy-Carbon Electrode (3 cm^2) in Water

entry	substrate	pH	E/V vs. SCE	time/h	amt of products/μmol				$\eta_{NH_3}{}^d$/%
					NH_3	N_2O	NO_2^-	H_2	
a	$NaNO_3{}^b$	10	−1.25	3	44.8	0	30.8	25.5	70.3
b	$NaNO_2{}^c$	7	−1.25	3	62.8	0		74.4	71.5
c		10	−1.25	3	46.4	0		10.1	88.9
d		12	−1.25	3	30.9	0		4.5	95.3
e		10	−1.20	3.4	29.5	0		3.8	85.4
f		10	−1.15	19.0	27.5	0.8		2.9	83.8
g		10	−1.10	40.5	0	8.2		70.2	0
h	$NH_2OH{}^c$	10	−1.25	3	135.1	0		32.4	80.6

^{a} 1.0×10^{-7} mol. ^{b} 5.0×10^{-2} mol dm^{-3}. ^{c} 5.0×10^{-3} mol dm^{-3}. ^{d} Current efficiency for the formation of NH_3.

Scheme II

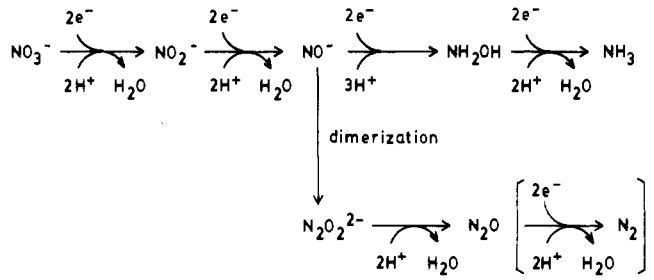

up around +0.3 V of E_r vs. SCE when E_d = −1.5 V vs. SCE and the ring current I_r increases with a shift in E_r to the positive side (curve b in Figure 6). Such anodic current may be assigned to the oxidation of NH_2OH produced in the reduction of NO_2^-, because curve b in Figure 6 was completely consistent with the I_r–E_r curve for an aqueous H_3PO_4–NaOH buffer solution of NH_2OH (pH 10) at the same RRDE. In addition, the reduction of NH_2OH (5.0×10^{-3} mol dm^{-3}) with the [Mo-Fe]/GC electrode by the electrolysis at −1.25 V vs. SCE in water (pH 10) smoothly proceeds to produce NH_3 and H_2 catalytically, as shown in entry h of Table I. These results indicate that NH_2OH is an intermediate in the reduction of NO_2^- to NH_3.

The results for the reduction of NO_2^- with the [Mo-Fe]/GC electrode under various conditions are summarized in Table I, which reveals that the amounts of H_2 and NH_3 formed in the reduction decrease with increasing pH value, whereas the current efficiency for the formation of NH_3 increases with increasing pH value (entries b–d in Table I); the current efficiency for the formation of NH_3 reaches 95.3% at pH 12. These results suggest that the reductions of NO_2^- and protons take place competitively. It should be noted that the reduction products are changed depending on the electrode potential (entries e–g in Table I); the reduction of NO_2^- at −1.20 V vs. SCE affords NH_3 together with H_2, being similar to that at −1.25 V vs. SCE (compare entry c with entry e in Table I), while a small amount of N_2O as well as NH_3 is produced in the reduction conducted at −1.15 V vs. SCE. A further anodic shift of the electrode potential to −1.10 V vs. SCE results in a complete depression of the formation of NH_3; instead, N_2O is formed as a reduction product (entry g in Table I). The alternation of the main product from NH_3 to N_2O in the reduction of NO_2^- suggests that both reductions proceed via a common reaction intermediate. A most plausible intermediate for the reduction of NO_2^- to NH_2OH is unstable NO^- (or NOH), which is known to dimerize rapidly in organic solvents, giving $N_2O_2^{2-}$ (or $N_2O_2H_2$).[37] The hyponitrite anion $N_2O_2^{2-}$, however, easily undergoes decomposition in water to afford N_2O.[38-40] The present N_2O evolution in the reduction of NO_2^- may, therefore, arise from the preferential dimerization of NO^- to $N_2O_2^{2-}$ rather than the reduction of NO^- to NH_2OH owing to a decrease of multielectron reductions caused by the anodic shift of the [Mo-Fe]/GC electrode potential.

Reduction Pathways of NO_3^- and NO_2^-. Possible reduction pathways of NO_3^- to NH_3 and N_2O are depicted in Scheme II. The reduction of NO_3^- with the [Mo-Fe]/GC electrode at −1.25 V vs. SCE proceeds via NO_2^-, NO^-, and NH_2OH successively to afford NH_3. The rate-determining step may be the reduction of NO_3^- to NO_2^-, since the latter is accumulated to some extent in the reaction mixture (Figure 3) and NH_2OH is not identified in the reaction products. On the other hand, when the reduction of NO_2^- was carried out at −1.10 V vs. SCE, the first reduction product of NO^- dimerizes to $N_2O_2^{2-}$ before it is reduced to NH_2OH. The resulting $N_2O_2^{2-}$ anion easily undergoes decomposition in water to evolve N_2O. Biologically dissimilatory reduction of NO_2^- has been suggested to produce N_2 via N_2O.[5] Although no N_2 evolution has taken place in the present NO_3^- and NO_2^- reductions, the controlled-potential electrolysis of an N_2O-saturated aqueous solution (pH 10) with the [Mo-Fe]/GC electrode at −1.25 V vs. SCE has evolved N_2 catalytically with a 50% current efficiency. Thus, the [Mo-Fe]/GC electrode can simulate the assimilatory and dissimilatory reductions of NO_3^- and NO_2^-. In addition, the reduction pathway of NO_3^- presented in Scheme II is consistent with that proposed for the reduction of NO_3^- by assimilatory and dissimilatory reductases.[3]

Acknowledgment. We are deeply indebted to the Japan Securities Scholarship Foundation for the support of this research.

Registry No. $(Bu_4N)_3[Mo\text{-}Fe]$, 68197-68-2; $[Mo\text{-}Fe]^{4-}$, 81276-61-1; $[Mo\text{-}Fe]^{5-}$, 76125-83-2; NO_3^-, 14797-55-8; NO_2^-, 14797-65-0; $NaNO_3$, 7631-99-4; $NaNO_2$, 7632-00-0; NH_2OH, 7803-49-8; NH_3, 7664-41-7; N_2O, 10024-97-2; H_2, 1333-74-0; C, 7440-44-0.

(37) Hughes, M. N. *Q. Rev., Chem. Soc.* **1968**, *22*, 1.
(38) Hughes, M. N.; Stedman, G. S. *J. Chem. Soc.* **1963**, 1239.
(39) Latimer, W. M.; Zimmermann, H. W. *J. Am. Chem. Soc.* **1939**, *61*, 1550.
(40) Buchholz, J. R.; Powell, R. E. *J. Am. Chem. Soc.* **1963**, *85*, 509.